

RESEARCH PAPER

Dynamics of aquaporins and water relations during hypocotyl elongation in *Ricinus communis* L. seedlings

Daniel A. Eisenbarth and Alfons R. Weig*

Department of Plant Physiology, University of Bayreuth, Universitätsstrasse 30, D-95447 Bayreuth, Germany

Received 13 August 2004; Accepted 29 March 2005

Abstract

The rate of water flow across biological membranes can be modulated by aquaporins which are expressed in many cells and tissues. The biological functions of these water channels in cellular processes have often been anticipated from the expression pattern, although the participation in the underlying process is not known in many cases. Ten putative aquaporin transcripts were identified in castor bean (*Ricinus communis* L.) seedlings and the water channel activity of three selected genes was analysed by heterologous expression in *Xenopus* oocytes, as well as the spatial and temporal expression by *in situ* hybridization/immunolocalization along the hypocotyl's axis. Water relations parameters were studied in elongating and non-elongating tissues using the cell pressure probe technique. These results indicate that (i) the amount of the RcPIP2-1 aquaporin correlated best with the elongation activity of the etiolated hypocotyl and (ii) the hydraulic conductivity of cortex cells is significantly higher in the elongating region of the hypocotyl compared with the non-elongating, mature region.

Key words: Aquaporin, growth, hydraulic conductivity, hypocotyl elongation.

Introduction

In plants, aquaporins are encoded in a large gene family, the major intrinsic proteins (MIP; Reizer *et al.*, 1993). The *Arabidopsis* genome harbours 35 MIP genes (Johanson *et al.*, 2001; Quigley *et al.*, 2002) which can be subdivided into four distinct subfamilies; the TIP and PIP subfamilies contain aquaporins of the tonoplast and the plasma

membrane, respectively (Höfte *et al.*, 1992; Kammerloher *et al.*, 1994). The NIP subfamily combines sequence motives of classical aquaporins and of glycerol permeases; members of this subfamily transport water and glycerol across membranes (Weig *et al.*, 1997; Dean *et al.*, 1999; Weig and Jakob, 2000). The subcellular localization of NIPs as well as of a fourth subfamily (small/basic intrinsic proteins: SIP) is unknown. Although the majority of PIPs and TIPs are quite specific for water, some transport other small molecules such as glycerol, urea, or carbon dioxide (Biela *et al.*, 1999; Gerbeau *et al.*, 1999; Uehlein *et al.*, 2003; Hanba *et al.*, 2004).

Aquaporins facilitate the diffusion of water molecules across membranes according to a water potential gradient. Therefore, the amount of active aquaporins will primarily determine the water conductivity of a membrane. Because the water permeability of the tonoplast is much higher compared with the plasma membrane (Maurel *et al.*, 1997), it is most likely the hydraulic conductivity of the plasma membrane which will determine the hydraulic conductance of the transcellular pathway in a tissue. In addition to transcriptional and translational control of aquaporin gene expression, post-transcriptional control of aquaporin activity by protein phosphorylation, pH-effects, and heteromeric assembly have been described recently (Maurel *et al.*, 1995; Johansson *et al.*, 1998; Tournaire-Roux *et al.*, 2003; Fetter *et al.*, 2004).

Whether aquaporins limit water transport across tissues is, however, still a matter of debate (Hill *et al.*, 2004). Many processes in plants exist which are dependent on massive water flow into and out of cells, such as uptake of water by roots, elongation growth, stomata and motor cell movements, or phloem transport (for reviews see Tyerman *et al.*, 1999; Maurel and Chrispeels, 2001). Shoot (stem) growth has been intensively investigated using the soybean hypocotyl

* To whom correspondence should be addressed. Fax: +49 921 55 842624. E-mail: alfons.weig@uni-bayreuth.de

(for review see Boyer and Silk, 2004). Most of the growth water is delivered to the growing tissue via the vascular system which is embedded deep inside the hypocotyl tissue. Water fluxes through the tissue surrounding the water-delivering xylem (and phloem) elements is considerably larger compared with cells of the periphery of the cortex because it has to take up water not only for its own growth but also to allow passage of water for growth of the outer tissue. Water flow is dependent on a water potential gradient and the direction of this gradient determines the direction of water flow. Radial water potential gradients have been described for the soybean hypocotyl which should be steepest close to the vascular system (Nonami *et al.*, 1997). It has been proposed that small cells close to the xylem mostly impede radial water flow in the growing hypocotyl.

The growing castor bean (*Ricinus communis* L.) hypocotyl is morphologically similar to the soybean hypocotyl although it does not form a continuous circular layer of metaxylem as in soybean. The castor bean seedling has been intensively used in the authors' laboratory to investigate long-distance transport processes of sugars, amino acids, and water (Kallarackal *et al.*, 1989; Schobert and Komor, 1989; Köckenberger *et al.*, 1997). In contrast to soybean (where assimilates are stored in the cotyledons), the primary storage tissue in castor bean seeds is the endosperm, a maternal tissue which releases assimilates apoplastically to the growing seedling. Because the endosperm can easily be removed and replaced by an artificial nutrient solution (Kallarackal *et al.*, 1989), this system offers the advantage of altering the assimilate supply to sink tissues in a defined way. Furthermore, the growing zone of the castor bean hypocotyl is preceded by a distinct 'pre-elongation' zone which is characterized by non-elongating, starch-filled cells. These cells continuously displace the cells of the elongation zone as they elongate to form the mature hypocotyl. Therefore, the hypocotyl axis represents a time scale where the onset and offset of processes during initiation and inhibition of cell elongation can be monitored. Similar to the soybean hypocotyl, the cortex of the castor bean hypocotyl also consists of about 15 cell layers. If radial water flux follows the trans-cellular path across the cortex, a hydraulic limitation of this flux should be easily detectable in this multi-layer tissue because a series of hydraulic resistances (series of cell membranes; Steudle, 1997) will determine the overall hydraulic conductance of the hypocotyl cortex. In addition, a gradient in water potential between periphery and vascular tissue could cause apoplastic tension resulting in water flux along the apoplastic path (Boyer, 2001). Finally, the elongation process can be rapidly stopped by illumination. This natural stimulus provides an endogenous 'switch' to manipulate water flow and to test the relevance of various parameters.

If aquaporins are necessary for radial water flow, it is expected that their temporal and spatial expression should

be correlated to growth rates along the hypocotyl axis and possibly be affected by the light-induced arrest of hypocotyl elongation. Using molecular techniques, a small family of MIP gene transcripts was identified in the hypocotyl tissue and their expression profile along the hypocotyl axis was analysed. The spatial expression of *RcPIP2-1*, which correlated best with the observed growth rates of the hypocotyl, was investigated by *in situ* hybridization and immunolocalization. Furthermore, radial profiles of hydraulic conductivities of cortex cells in the growing and the mature hypocotyl as well as in growth-arrested hypocotyl cells were obtained using the cell pressure probe.

Materials and methods

Plant material and growth conditions

Ricinus communis L. var. 'Carmencita Rot' (Fa. Benary, Hannoversch Münden, Germany) was grown on sterile vermiculite or in hydroponics in the dark at 27 °C for 6–8 d as described previously (Kallarackal *et al.*, 1989). Inhibition of hypocotyl elongation (photomorphogenesis) was induced by illumination of the seedlings in a growth chamber with a light density of about 200 $\mu\text{E m}^{-2} \text{s}^{-1}$. To quantify growth along the hypocotyl axis, 6-d-old seedlings were marked with permanent ink (Staedler Lumocolor, Germany) in 5 mm intervals on day six after germination. The diameter and the length of each segment were measured after 24, 48, and 72 h and the volume of the hypocotyl cylinder was calculated.

Cloning of MIP transcripts by RT-PCR and library screening

MIP transcripts were amplified using cDNA preparations from cotyledons, hypocotyl, roots, and the endosperm of 6-d-old etiolated castor bean seedlings. Reverse transcription and amplification was performed as described previously (Weig *et al.*, 1997) using Superscript II reverse transcriptase (Invitrogen, Karlsruhe, Germany) and AmpliTaq polymerase (Applied Biosystems, Darmstadt, Germany). Primer pairs used for PCR amplification were TIP2/TIP4 (Weig *et al.*, 1997) and TIP4/TIP5 (TIP5: 5'-WSWYCTWG-CYGGRTTSAT). PCR fragments ranging from 363 to 450 base pairs were cloned into pTA6 vector (NCBI accession number AY454397), a pBluescript II SK⁺ derivative suitable for TA cloning. This vector was constructed by inserting a 39 bp double-stranded DNA fragment containing two *Xcm*I restriction sites into the *Eco*RI site of pBluescript II SK⁺. The double-stranded DNA was obtained by self-annealing of the 39 mer oligonucleotide (5'-AATTCGC-CAAGCCTGAGCTGGWCCAGCTCAGGCTTGGCG) which results in a DNA fragment containing two *Eco*RI compatible overhangs at each end. For TA-cloning, the resulting vector pTA6 was cut with *Xcm*I, dephosphorylated, and run on an agarose gel to separate the vector fragment (with a T-overhang on both end) from the stuffer fragment. Recombinant plasmids containing putative MIP cDNA fragments were analysed by restriction digest with *Eco*RI. In addition, the cDNA fragments of recombinant plasmids were PCR amplified using M13 forward and reverse sequencing primers and the amplified inserts were digested with the four base cutters *Sau*3AI and *Dde*I, respectively. Comparison of these restriction patterns allowed different gene transcripts to be distinguished and the number of clones for subsequent sequence analysis to be narrowed down.

Full-length cDNAs for *RcTIP1-1*, *RcPIP1-1*, and *RcPIP2-1* were identified by plaque screening of a cDNA library prepared in λ ExCell (Amersham Biosciences, Freiburg, Germany) from hypocotyl

tissue of 6-d-old seedlings (C Schobert and E Komor, unpublished results). The cDNA fragments were cloned into pBluescript II KS⁺ via the *EcoRI/NotI* restriction sites yielding plasmids pP2L, pP5L, and pT4L encoding RcPIP1-1, RcPIP2-1 and RcTIP1-1, respectively. The full-length fragments were sequenced on both strands.

RNA extraction and analysis

RNA was extracted using the FastRNA-Pro Green kit together with Lysing Matrices D (Q-Biogene, Heidelberg, Germany) in an automatic homogenizer (FastPrep-Instrument; Q-Biogene, Heidelberg, Germany) following the manufacturer's recommendations. Total RNA (9 µg) was separated on a 1.2% (w/v) agarose gel containing formaldehyde, and transferred onto nylon membranes. All hybridizations were carried out using the digoxigenin non-radioactive labelling and detection system (Roche Diagnostics, Mannheim, Germany), including a DIG RNA labelling kit for preparing the gene-specific sense or antisense probe, respectively. Detection was performed using NBT/BCIP (Roche Diagnostics, Mannheim, Germany) as the substrate for the alkaline phosphatase.

Protein extraction and immunological analysis

Antibodies against the different aquaporins are directed against short peptides selected from the deduced amino acid sequence and were produced by Eurogentec (Seraing, Belgium) and Pineda Antikörper-service (Berlin, Germany). The peptide sequences used for the immunization of rabbits were: RNIAVGHPHEATQPDALK (located at the N-terminus of RcTIP1-1), GFEGSHDYTRLGGC (located in the central loop of RcPIP1-1, separating transmembrane helices 3 and 4), and VGEETQTSHGKC (located at the N-terminus of RcPIP2-1). Specific antibodies were affinity-purified from the crude blood sera using the peptides described above coupled to CNBr-activated Sepharose 4B (Amersham Biosciences, Freiburg, Germany). The antibodies were allowed to bind to the peptide-Sepharose beads for at least 12 h at 4 °C and eluted using 50 mM glycine (dissolved in water, resulting in a pH of 1.9) at room temperature; the eluted antibodies were immediately neutralized with 0.1 volume of 1 M TRIS/HCl (pH 8.0) and BSA was added to a final concentration of 1% (w/v). Microsomal membrane proteins were isolated from the three hypocotyl zones as described previously (Daniels *et al.*, 1994). Ten µg microsomal proteins were separated on a SDS-polyacrylamide gel and transferred electrophoretically on PVDF membranes. The membranes were blocked in PBS buffer (Sambrook *et al.*, 1989) containing 1% (w/v) low-fat milk powder and subsequently incubated with the affinity purified primary antibodies (1:500 dilution) and the secondary anti-rabbit antibody coupled to alkaline phosphatase (1:2000 dilution; monoclonal antibody RG-16, Sigma, Taufkirchen, Germany). The immunoblot was developed using NBT/BCIP (Roche Diagnostics, Mannheim, Germany) as the substrate for the alkaline phosphatase as recommended by the manufacturer.

Functional expression of MIPs in *Xenopus oocytes*

Full-length cDNA sequences were cloned in between the 5' and 3' *Xenopus* β-globin non-translated regions in a pSP64T-derived Bluescript vector (Preston *et al.*, 1992). *In vitro* transcribed and capped cRNA (m7G[5']ppp[5']G; New England Biolabs, Frankfurt, Germany) was injected into *Xenopus oocytes* (120 ng per oocyte), and incubated at 16 °C for 3 d in ND96 medium (Tang *et al.*, 2000), which was exchanged once a day. Oocyte swelling was video captured after the dilution of the incubation medium with distilled water. The initial volume, surface area, and increase in volume of each oocyte was measured using an image analysis software (Image-Pro Plus, Media Cybernetics Inc., USA) and used to calculate the osmotic water permeability as described previously (Weig *et al.*, 1997).

In situ hybridization

In situ hybridization was performed as described in the protocol available online from the Meyerowitz laboratory (<http://www.its.caltech.edu/~plantlab/protocols/insitu.htm>). The above protocol was adopted to the digoxigenin non-radioactive detection system (Roche) as recommended by the manufacturer (see the Non-radioactive *in situ* hybridization application manual, Roche Diagnostics, Mannheim, Germany); the most important changes were the use of a formalin-acetic acid mixture for fixation, a proteinase K treatment of only 15 min, and the use of levamisole (0.1 mM) but not polyvinyl alcohol in the detection reaction. The thickness of the sections was 8 µm. Specific probes for *RcPIP2-1* were digoxigenin labelled by *in vitro* transcription using T3 and T7 RNA polymerases on a plasmid containing the C-terminal part and the 3' non-translated region of *RcPIP2-1* as described in the instruction manual mentioned above.

Immunolocalization

Hypocotyl tissues were fixed and paraffin embedded as described for *in situ* hybridization. Sections of 8 µm were dewaxed, rehydrated, and incubated in blocking buffer made of 1% (w/v) low-fat milk powder in PBS buffer (Sambrook *et al.*, 1989) for 45 min. Affinity-purified polyclonal antibodies were diluted 1:200 in blocking buffer and the slides were incubated for 90 min. The primary antibodies were washed off with blocking buffer containing 0.1% (v/v) Tween 20 (Sigma), equilibrated in blocking buffer and incubated with the alkaline phosphatase coupled secondary antibody (monoclonal antibody RG-16, Sigma) for 60 min. Unbound antibodies were washed off with blocking buffer containing 0.1% (v/v) Tween 20. Staining of the sections was performed using NBT/BCIP as described in the digoxigenin labelling and detection manual (Roche) until visible colour precipitates had been formed. The phosphatase reaction was stopped by washing the slides in distilled water; the colour was preserved by mounting the sections in AquaTex (VWR International, Darmstadt, Germany).

Quantification of transcript and protein amounts

Transcript and protein amounts of RcTIP1-1, RcPIP1-1, and RcPIP2-1 on gel blots were quantified using the 'ImageMaster 1D' gel analysis software (version 3; Amersham Biosciences, Freiburg, Germany). The background surrounding each single band was subtracted before quantification of each signal.

The spatial signal intensity derived from *in situ* hybridizations and immunolocalizations was quantified using the 'ImagePro Plus' software (version 4.5; Media Cybernetics, Silver Spring, MD, USA). A rectangular section of each picture was selected and the average pixel value was calculated by the software in radial direction.

Cell pressure probe measurements

All pressure probe measurements were carried out in a room which could be completely darkened. To observe the insertion and manipulation of the glass capillary of the cell pressure probe into hypocotyl cells 'in the dark', photomorphogenic inactive green light in combination with a far-red light was used during the experiment using etiolated seedlings; a white light source (KL 1500; Schott, Mainz, Germany) was equipped with two flexible light guides carrying the following filters: a longpass filter (RG715, Itos, Mainz, Germany) allowing the passage of far-red light above 715 nm, and a bandpass filter (D525/50; AHF Analysentechnik, Tübingen, Germany) allowing the passage of green light ranging from 500 to 550 nm. To inhibit hypocotyl elongation etiolated seedlings were illuminated as described above and kept continuously under white light throughout the experiment.

The cell pressure probe (Hüsken *et al.*, 1978) was used as described previously (Henzler *et al.*, 1999). The castor bean seedlings

were carefully fixed with a soft clamp and covered with wet tissue paper to avoid transpiration; the roots were kept in 0.5 mM CaCl₂ throughout the experiment. The pressure probe was filled with de-gassed silicon oil (AS4, Wacker Chemie, Stuttgart, Germany) and connected to a computer via an analog-to-digital converter (Type 92101, Burster Präzisionsmesstechnik, Gernsbach, Germany). Colour markings on the glass capillary were used to determine the position of the tip of the capillary inside the cortex tissue. The measurements were recorded and analysed using the PFLOEK software package (version 1.06) developed by Ernst Steudle and co-workers (University of Bayreuth).

Turgor pressure (P) was changed by the help of a motor-driven micrometer within less than one second to induce water flow into and out of cells. The hydraulic conductivity (Lp) was calculated from hydrostatic pressure relaxations according the following equation:

$$Lp = V/A \times \ln(2) / [T_{1/2} \times (\epsilon + \pi^i)] \quad (\text{Hüsken } et al., 1978)$$

where V represents the cell volume, A the surface area, and π^i the osmotic pressure of the cell sap which was deduced from the stationary turgor at zero water potential. The elastic modulus (ϵ) was calculated according

$$\epsilon = V(\Delta P / \Delta V) \quad (\text{Hüsken } et al., 1978)$$

The surface area of cells across the cortex could not be measured directly but was deduced from cross and longitudinal sections (50 μ m thickness) of the hypocotyl tissue. The cortex tissue in the different zones was divided into 15 intervals (the investigated region in the cortex represented about 15 cell layers) and average length and diameter were calculated from about 500 individual measurements for each interval. The trend line of the cortical profiles was used to select the mean values of V and A for each individual pressure probe measurement. For statistical analysis of water relations parameters, measurements were grouped into four depth intervals. In each depth interval, three pairs of data (elongation zone versus mature zone, elongation zone versus arrested elongation zone, mature zone versus arrested elongation zone) were analysed using the Mann-Whitney Rank-Sum-Test (SigmaStat version 3.1, Systat Software GmbH, Erkrath, Germany).

Results

Growth characteristics of the castor bean hypocotyl

Elongation growth of etiolated castor bean hypocotyls is mainly restricted to a short region below the hypocotyl hook (Fig. 1A) which can be rapidly inhibited by light (Fig. 1C). By contrast, growth of the apical part of the hypocotyl is mainly due to cell division as it can be seen on cross-sections (data not shown). During cell pressure probe experiments 'in the dark', the seedlings were illuminated with non-photomorphogenically active green and far-red light, which did not inhibit hypocotyl growth (cells of the hypocotyl hook continue to replace cells of the elongation zone; Fig. 1D, E). The analysis of the length and diameter of hypocotyl segments of the elongation zone and the growth-arrested elongation zone as well as the mature hypocotyl indicated that the hypocotyl segment just below the hypocotyl hook grew significantly faster compared with segments of the mature hypocotyl or the growth-arrested elongation zone of seedlings in the light (Fig. 1F).

Abundant aquaporin gene transcripts in the hypocotyl

Since aquaporins are encoded in a large gene family in many plant species, degenerate primers were used to amplify aquaporin gene fragments from different tissues of castor bean. RT-PCR using the primer combination TIP2/TIP4 (Weig *et al.*, 1997) or TIP4/TIP5 (this work) amplified cDNA fragments of putative TIP and PIP genes of 363, 422, and 452 bp, respectively. The fragments were ligated to the TA-cloning vector pTA6. Careful inspection of the restriction pattern of 104 independent plasmids and DNA sequence analysis of 20 selected plasmids revealed

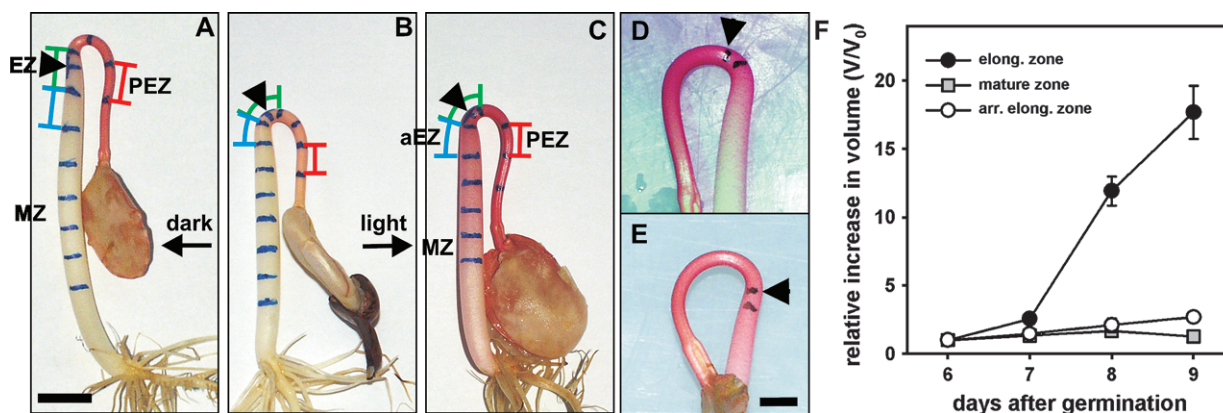


Fig. 1. *Ricinus communis* L. seedlings. 6-d-old seedlings were grown in the dark (B) and marked with ink on top of the hypocotyl hook (triangle in B); 2.5 mm acropetal and basipetal of this marking were selected as the initial segment (green segment), from which additional 5 mm segments were marked towards the roots and the shoots. Seedlings were either kept in the dark (A) or transferred to the light (C) for an additional 12 h. During hypocotyl growth in the dark, the region basipetal to the hypocotyl hook (blue segment in A) elongates and is continuously replaced by the tissue of the hypocotyl hook (green segment in A). In the light, hypocotyl elongation is greatly reduced; the former elongation zone shows only little elongation (blue segment in C) and is not replaced by the tissue of the hypocotyl hook (green segment in C). Tissues analysed in this work were from the pre-elongation zone (PEZ), the elongation zone (EZ) or the growth-arrested elongation zone (aEZ), and the mature zone (MZ) of dark-grown and illuminated seedlings. Water relations parameters were analysed in EZ and MZ of dark-grown seedlings and in aEZ of illuminated seedlings. Non-photomorphogenic light used for cell pressure probe experiments did not inhibit hypocotyl elongation (D, E: before and after 12 h of illumination by green and far-red light, respectively). Scale bars: 1 cm. Relative increase in volumes of hypocotyl segments (EZ, MZ, and aEZ) from 6–9 d after germination are given in (F).

that these cDNA fragments represented transcripts from eight independent *MIP* genes of *Ricinus communis* (Table 1). A BLAST database search using TIP and PIP protein sequences from *Arabidopsis* against *Ricinus communis* entries in the EST database section at NCBI (<http://www.ncbi.nlm.nih.gov/>) identified two additional *MIP* gene transcripts closely related to plant TIP genes (van de Loo *et al.*, 1995; see Table 1). Sequence comparison of the deduced peptide sequences of all castor bean *MIP* cDNA clones to the *MIP* family of *Arabidopsis* (Johanson *et al.*, 2001) let gene names be selected which indicate the relationship of each *Ricinus MIP* gene to the most similar subgroup within the *Arabidopsis MIP* family, for example, RcPIP1-1 is very similar to the PIP1 subgroup of *Arabidopsis* while RcPIP2-1 is similar to the PIP2 subgroup (Table 1). The second number in the gene names indicates a specific *MIP* within a subgroup as proposed previously (Johanson *et al.*, 2001).

A series of independent RNA gel blot hybridizations was performed with each of the ten *Ricinus MIP* cDNA clones in order to identify abundant aquaporin transcripts and (at a first approximation) abundant aquaporin proteins in castor bean. *RcTIP1-1*, *RcPIP1-1*, and *RcPIP2-1* were the major abundant *MIP* transcripts in hypocotyl tissue, and hybridization signals from other *MIP* transcripts were less than 10% compared with the *RcTIP1-1* transcript in this organ (data not shown). The two *MIP* clones (pCRS661 and pCRS831; Table 1), which were identified in germinating castor bean seedlings (van de Loo *et al.*, 1995), turned out to be hardly expressed in hypocotyl tissue. These two *Ricinus MIP* genes are obviously orthologous proteins closely related to α -TIPs (TIP3 subgroup; Johanson *et al.*, 2001) from *Phaseolus vulgaris* (Johnson *et al.*, 1990) and *Arabidopsis* (Höfte *et al.*, 1992), which are exclusively expressed during seed development and germination. Since

RcTIP1-1, *RcPIP1-1*, and *RcPIP2-1* represented the most abundant *MIP* transcripts in castor bean hypocotyl extracts, full-length cDNA clones of these three transcripts were isolated from a cDNA library prepared from hypocotyl tissue of castor bean using the corresponding PCR fragments as the hybridization probes (Table 1). When the entire protein sequence was compared with the *Arabidopsis* MIPs, RcTIP1-1 exhibits highest similarity to AtTIP1-1 (γ TIP), a tonoplast aquaporin which is predominantly expressed in the elongation zone of *Arabidopsis* roots (Ludevid *et al.*, 1992). RcPIP1-1 is very similar to AtPIP1-4 (TMP-C), which has been originally isolated from *Arabidopsis* flower buds (Kinoshita *et al.*, 1994). Finally, RcPIP2-1 is closely related to AtPIP2-7 and AtPIP2-8, which are not yet described in detail.

Functional expression of castor bean aquaporins in *Xenopus oocytes*

To investigate the aquaporin activity of the RcTIP1-1, RcPIP1-1, and RcPIP2-1, corresponding cRNA was injected in oocytes. *RcTIP1-1* and *RcPIP2-1* injected oocytes exhibited significantly increased osmotic water permeability compared with water-injected oocytes (Fig. 2). *RcPIP1-1* injected oocytes exhibited swelling rates indistinguishable from water-injected oocytes (data not shown). Therefore it remains to be investigated whether RcPIP1-1 is able to form a functional water channel or whether this protein is dependent on a heteromeric assembly as has been described for other PIP1 aquaporins (Fetter *et al.*, 2004).

Expression profile of abundant *MIP* transcripts along the hypocotyl axis

To relate the expression profile of castor bean *MIP* genes with the elongation activity along the hypocotyl axis, three zones along the hypocotyl axis (the pre-elongation zone, the elongation zone, and the mature hypocotyl; see Fig. 1) were investigated in detail. RNA gel blot hybridizations

Table 1. *MIP* transcripts and nomenclature in *Ricinus communis*

Plasmid	NCBI accession number	Gene name in <i>Ricinus communis</i>	Closest <i>Arabidopsis</i> orthologue ^d
pR450-16 ^a	AJ605566	<i>RcPIP1-1</i>	<i>AtPIP1-4</i>
pP2L ^b	AJ605574		
pR450-14 ^a	AJ605567	<i>RcPIP1-2</i>	<i>AtPIP1-1</i>
pR450-8 ^a	AJ605569	<i>RcPIP2-1</i>	<i>AtPIP2-8</i>
pP5L ^b	AJ605575		
pR450-3 ^a	AJ605565	<i>RcPIP2-2</i>	<i>AtPIP2-4</i>
pR450-4 ^a	AJ605568	<i>RcPIP2-3</i>	<i>AtPIP2-2</i>
pR450-17 ^a	AJ605571	<i>RcTIP1-1</i>	<i>AtTIP1-1</i>
pT4L ^b	AJ605573		
pR450-12 ^a	AJ605570	<i>RcTIP1-2</i>	<i>AtTIP1-3</i>
pCRS661 ^c	T15177	<i>RcTIP3-1</i>	<i>AtTIP3-2</i>
pCRS831 ^c	T15236	<i>RcTIP3-2</i>	<i>AtTIP3-2</i>
pR450-22 ^a	AJ605572	<i>RcTIP4-1</i>	<i>AtTIP4-1</i>

^a Partial cDNA clone (this work).

^b Full-length cDNA clone (this work).

^c EST clones (van de Loo *et al.*, 1995).

^d Johanson *et al.* (2001).

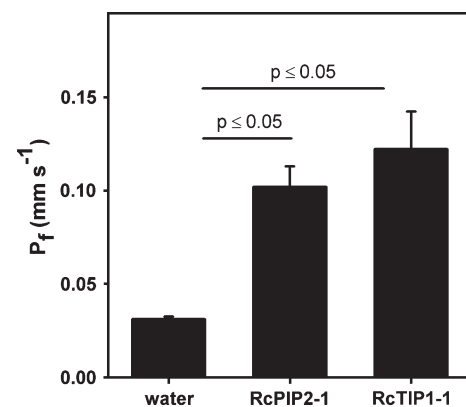


Fig. 2. Osmotic water permeability of *Xenopus* oocytes injected with sterile water or with cRNA of *RcPIP2-1* and *RcTIP1-1*, respectively. The P_f values are expressed as means \pm SE ($n=10$).

with digoxigenin labelled probes of *RcTIP1-1*, *RcPIP1-1*, and *RcPIP2-1*, respectively, showed that in etiolated seedlings the amount of these *Ricinus MIP* transcripts is higher in cells of the elongation zone compared with the pre-elongation zone (Fig. 3A–C). The amount of *RcTIP1-1* and *RcPIP2-1* mRNA is reduced after the elongation phase (Fig. 3A, C) while *RcPIP1-1* mRNA remains at the high level (Fig. 3B). Illumination of etiolated *Ricinus* seedlings rapidly inhibits the elongation process and induced photomorphogenesis (Fig. 1). In the light, no increase in the amount of any of the three aquaporin transcripts in cells of the former elongation zone could be observed (Fig. 3A–C). Quantification of the RNA hybridization signals (Table 2) confirmed the observation that (i) *RcTIP1-1* expression did not change very much, (ii) *RcPIP2-1* mRNA is increased in the elongation zone and in the light, and (iii) that the mRNA profile of *RcPIP2-1* is transiently increased in the elongating hypocotyl but not in the mature hypocotyl nor in the light.

To investigate whether the increased amounts of *MIP* mRNA will increase the amounts of corresponding proteins during elongation, microsomal proteins from the different hypocotyl zones were separated under denaturing conditions, transferred on to membranes, and incubated with antibodies directed against short peptides of *RcTIP1-1*, *RcPIP1-1*, and *RcPIP2-1* (Fig. 3E–G). A significant increase of aquaporin density along the hypocotyl axis could be observed only for *RcPIP2-1* in the dark (Fig. 3G; Table 2). In contrast to the transient increase of *RcPIP2-1* mRNA in dark-grown seedlings (Fig. 3C), the *RcPIP2-1* protein increase was not transient but remained at high levels in the

mature hypocotyl (Fig. 3G). In illuminated seedlings, accumulation of *RcPIP2-1* protein was observed neither in the elongation zone nor in the mature hypocotyl. Although *RcTIP1-1* and *RcPIP1-1* mRNA (based on equal amounts of total RNA used in the RNA gel) accumulated in the elongation zone, the corresponding protein amount (based on equal amounts of microsomal protein used in the protein gel) did not change significantly (Fig. 3E, F). Quantification of the antibody-stained protein gel blots confirmed that *RcPIP2-1* exhibited relatively the largest changes in protein amount along the hypocotyl axis in dark-grown *Ricinus* seedlings (Table 2).

In situ hybridization of *RcPIP2-1*

Since the mRNA profile of *RcPIP2-1* was closely correlated to the elongation activity of the hypocotyl cells, the spatial expression of this gene was investigated by *in situ* hybridization along the hypocotyl axis. *RcPIP2-1*-specific hybridization signals were observed on cross-sections of the pre-elongation and the elongation zones in small cells of the vascular bundle, as well as in cells of the cortex close to the epidermis (Fig. 4A, B). These hybridization signals were not detectable on cross-sections of the mature hypocotyl and in the growth-arrested elongation zone of illuminated seedlings (Fig. 4C, E). Interestingly, hybridization signals in peripheral cells on cross-section of the pre-elongation zone and the hypocotyl hook were more intense on that side of the hypocotyl, which formed the outer side of the hook (red arrows in Fig. 4A, D). Quantification of the hybridization signals by densitometry analysis showed that

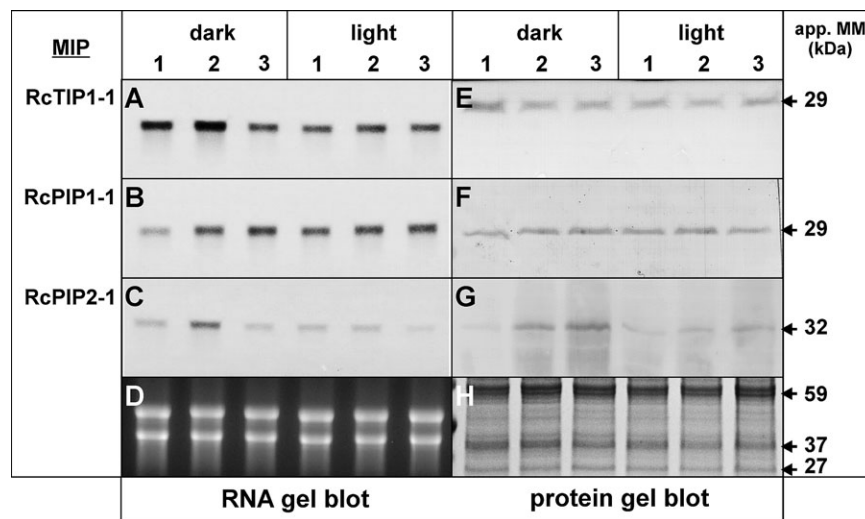


Fig. 3. mRNA and protein levels of *RcTIP1-1*, *RcPIP1-1*, and *RcPIP2-1* along the hypocotyl axis of developing *Ricinus* seedlings. RNA gel blots were hybridized using probes specific for *RcTIP1-1* (A), *RcPIP1-1* (B), and *RcPIP2-1* (C), respectively. Protein gel blots of hypocotyl membrane proteins were stained with peptide-specific antibodies against *RcTIP1-1* (E), *RcPIP1-1* (F), and *RcPIP2-1* (G); RNA and protein samples were isolated from the pre-elongation zone (1), the elongation zone (2), and from the mature hypocotyl (3) from dark-grown plants and from plants which were illuminated for 12 h. Parts of the underlying RNA gel (stained with ethidium bromide) and the protein gel (stained with Coomassie blue) are shown in (D) and (H). The RNA and protein analyses were repeated at least three times and representative results are shown. The apparent molecular mass of the antibody-specific signals and of some prominent bands of the Coomassie-stained gel is shown on the right (for quantification of these blots see Table 2).

Table 2. Quantification of mRNA–protein amounts of *RcTIP1-1*, *RcPIP1-1*, and *RcPIP2-1* along the hypocotyl axis (see Fig. 3)

The intensity values of the pre-elongation zone of etiolated seedlings were used as a reference and were set to 1.

Growth condition		Dark			Light		
		1	2	3	1	2	3
Hypocotyl segment							
RcTIP1-1	mRNA	1	1.21	0.65	0.58	0.65	0.62
	protein	1	0.49	0.48	0.44	0.35	0.61
RcPIP1-1	mRNA	1	2.40	2.76	2.12	2.54	2.64
	protein	1	1.20	1.46	1.22	1.49	1.00
RcPIP2-1	mRNA	1	2.71	0.62	0.78	0.88	0.45
	protein	1	4.15	6.24	1.35	1.56	2.93

the hybridization signal of peripheral cells is indeed asymmetric in the pre-elongation zone but symmetric in the elongation zone (red arrows in Fig. 4A' and B'; please note that the darker picture areas are represented by lower pixel values). By contrast, the *RcPIP2-1*-specific staining of small cells in between the xylem and the phloem was symmetric in all hybridizations of dark-grown seedlings (green arrows in Fig. 4A, B, C, and in the corresponding pixel intensity profiles).

Immunolocalization of *RcPIP2-1*

Immunolabelling of sections of the pre-elongation zone, the elongation zone, and the mature hypocotyl using peptide-specific antibodies against *RcPIP2-1*, showed specific labelling of cells within the vascular bundle and between the bundles, which was strongest in cross-sections of the elongation zone, but also detectable in the pre-elongation zone (Fig. 5D, E). In control experiments, staining of these cells disappeared when the antibodies were preincubated with an excess of soluble *RcPIP2-1* peptide, which was used for the immunization of rabbits (Fig. 5A, B). It was hardly detectable in vascular cells of the mature hypocotyl zone and of illuminated seedlings (Fig. 5C, E). In good agreement with the *in situ* hybridization results (Fig. 4), these cells probably represent pre-cambial cells as well as xylem and phloem parenchyma cells (red arrows in Fig. 5B). Phloem cells which could be clearly identified using antibodies directed against a phloem-localized sucrose carrier (Eisenbarth and Weig, 2005) were not stained with the anti-*RcPIP2-1* antibody. Unfortunately, four independent immunizations of rabbits resulted in antibodies with considerable high background, which made a precise investigation of *RcPIP2-1* localization in the cortex and pith tissue difficult. Comparison of radial intensity profiles of Fig. 5B and D (elongation zone of etiolated and illuminated seedlings, respectively) indicated that the signals within the vascular bundle were significantly different ($P \leq 0.001$) between etiolated and illuminated seedlings. In the cortex, however, no significant difference was observed between these two growth conditions ($P=0.695$).

Incubation of hypocotyl sections using antibodies directed against *RcTIP1-1* and *RcPIP1-1* showed intensive staining across the entire cross-section, which did not change along the hypocotyl axis or after illumination. Because the preimmune sera did not stain these cross-sections it is assumed that these two MIPs are abundant in the castor bean hypocotyl, but their protein profile does not correlate with hypocotyl elongation (data not shown).

Cell pressure probe measurements

To compare the water permeability of rapidly elongating versus non-elongating hypocotyl regions, hydraulic parameters were measured in three different regions using the cell pressure probe: (i) in the elongation zone of etiolated seedlings, (ii) the mature non-elongating zone of etiolated seedlings, and (iii) the growth-arrested elongation zone of illuminated seedlings (Fig. 6). When the cell pressure probe was inserted into etiolated seedlings, the plants were handled 'in the dark' under non-photomorphogenic green and far-red light. Control experiments have shown that these two light sources did not inhibit hypocotyl elongation (Fig. 1D, E).

An important parameter to calculate the water permeability of plant cells using the cell pressure probe is the surface area of the particular cell. Since collecting water transport parameters from several cells in a radial direction during the same experiment had been attempted by pushing the capillary deeper into the next cell layer after each measurement, the actual size of the cells could not be determined directly. To obtain cell dimensions of the three investigated zones, the hypocotyl was sectioned in the elongation zone (etiolated and illuminated seedlings) and in the mature hypocotyl tissue (etiolated seedlings) in both a radial and a longitudinal direction. Cortical cells exhibited a more or less cylindrical shape in cross-sections; therefore the volume and surface area were determined from two parameters, the diameter and the length of the cells. These two parameters were measured in about 1500 cells of the elongation and the mature zone of dark-grown seedlings and in the arrested elongation zone of illuminated seedlings (Fig. 7). Interestingly, cell volumes within the arrested elongation zone (illuminated seedlings) were only slightly larger compared with those of the elongation zone in dark-grown seedlings, but the diameter of this hypocotyl region was significantly thicker compared with the elongating hypocotyl (Fig. 7). This indicates that radial expansion of the cortex tissue was less inhibited compared with longitudinal growth.

In the outer cell layers the hydraulic conductivity (L_p) was significantly higher in the elongating hypocotyl compared with the mature hypocotyl (Fig. 6D). In addition, a 12 h illumination period reduced the L_p in peripheral cells of the former elongation zone to the same low L_p values which were found in mature hypocotyl cells of etiolated seedlings.

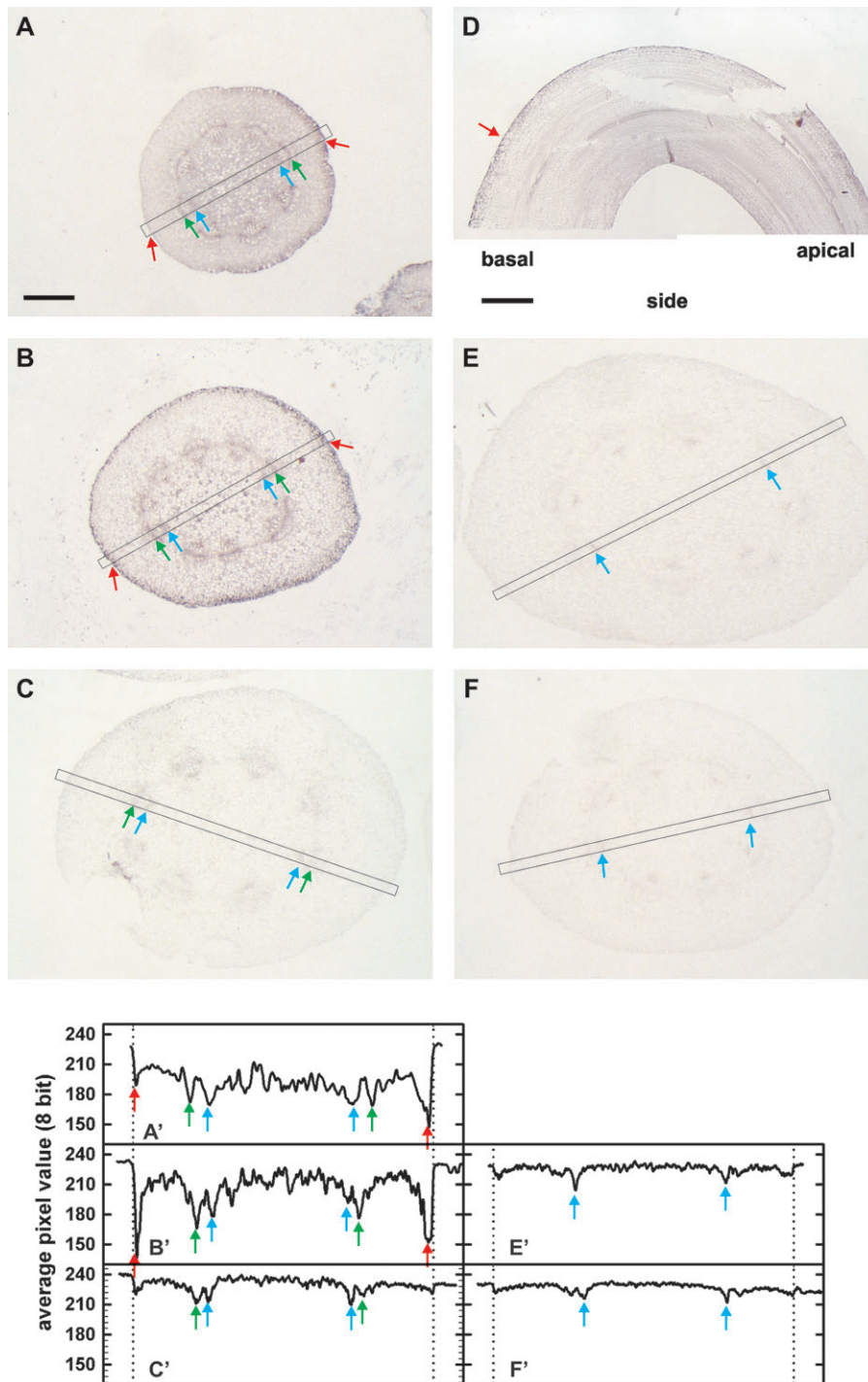


Fig. 4. *In situ* hybridization of cross-sections and longitudinal sections of the castor bean hypocotyl using *RcPIP2-1* specific probes. The sections were prepared from etiolated seedlings out of the pre-elongation zone (A), the elongation zone (B, F), the mature hypocotyl (C), and from the hypocotyl hook (D, longitudinal section, basal and apical side as indicated). An etiolated seedling was illuminated for 12 h and a cross-section from the growth-arrested elongation zone was used in (E). Antisense probes were used in (A–E) and a sense probe was used in (F). Red arrows indicate the predominant staining of peripheral cells in the pre-elongation zone (A), the hypocotyl hook (D), and the elongation zone (B); green arrows point to staining of vascular parenchyma cells. Quantification of the hybridization signals for each cross-section (see Materials and methods) is shown at the bottom and indicated by A', B', C', E', and F'. For better comparison, the length of the different profiles were scaled such that the surface of each cross-section is positioned at the dotted vertical line. The boxes in each picture indicate the regions used for quantification. Red and green arrows are as described above; blue arrows indicate the position of xylem elements in each single profile. Scale bar: 500 μm (1 mm in D).

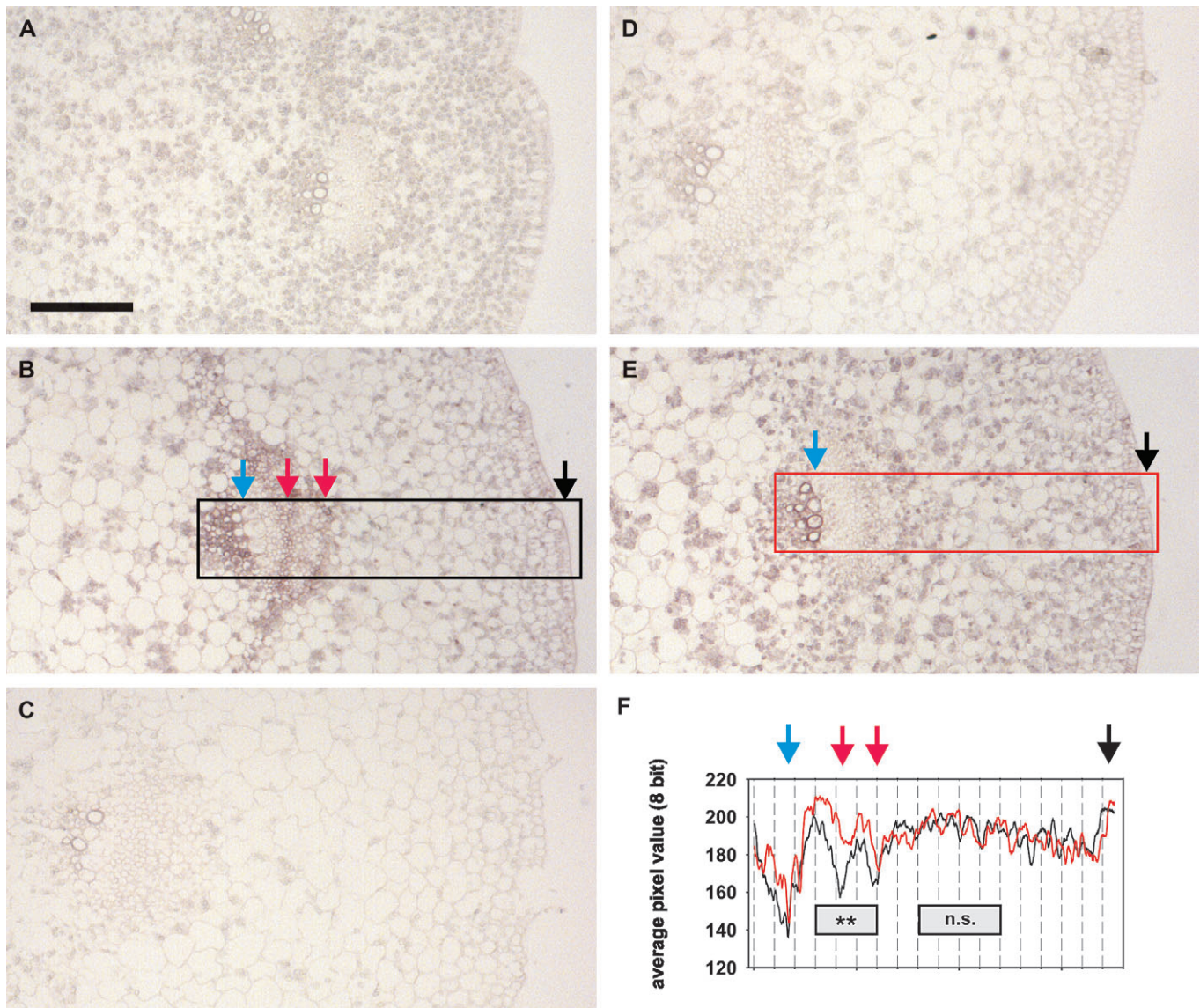


Fig. 5. Immunolocalization of the castor bean aquaporin RcPIP2-1 on cross-sections along the hypocotyl axis: The sections were prepared from the pre-elongation zone (A), the elongation zone (B, D), and the mature hypocotyl (C) of etiolated seedlings and from the growth-arrested elongation zone of illuminated seedlings (E). Cross-sections were incubated with affinity purified antibodies directed against RcPIP2-1 (A–C, E) or with the same antibody solution saturated with soluble RcPIP2-1 peptide used for immunization as a control (D). RcPIP2-1 specific staining was observed in parenchyma cells of vascular bundles in the elongation zone (red arrows in B) but not in the control incubation (D) and to a significantly lesser extent in the arrested elongation zone of illuminated seedlings (E). Quantification of the antibody signals (F) were performed using the two regions marked with boxes in (B) and (E). The two intensity profiles were aligned at the position of the xylem elements. Significant differences of the average pixel intensities between etiolated and illuminated seedlings within the vascular bundle or the cortex tissue (see boxes in F) were calculated using the Mann-Whitney Rank-Sum-Test ($n=40$); the significance levels were: $P \leq 0.001$ (**); ns=not significant. Scale bar: 500 μm .

Interestingly, a statistically significant radial gradient in turgor (P) could be observed in the elongating hypocotyl (Fig. 6A; P in depth interval 100–250 versus 550–700 μm : $P=0.038$; P in depth interval 250–400 μm versus 550–700 μm : $P=0.043$). Elongating cells exhibited in general a low elastic modulus (ϵ) compared with mature and illuminated cells (Fig. 6B). Although the half-time of pressure relaxation ($T_{1/2}$) seems to be shorter in elongating cells versus non-elongating cells, a statistically significant difference could only be proven between the elongating versus the

mature zone of etiolated seedlings in one of the depth intervals (Fig. 6C).

Discussion

RT-PCR cloning and the subsequent database search led to the identification of ten homologous gene transcripts of putative plant plasma membrane and tonoplast aquaporins (Table 1). Three of these genes, named *RcTIP1-1*, *RcPIP1-1*,

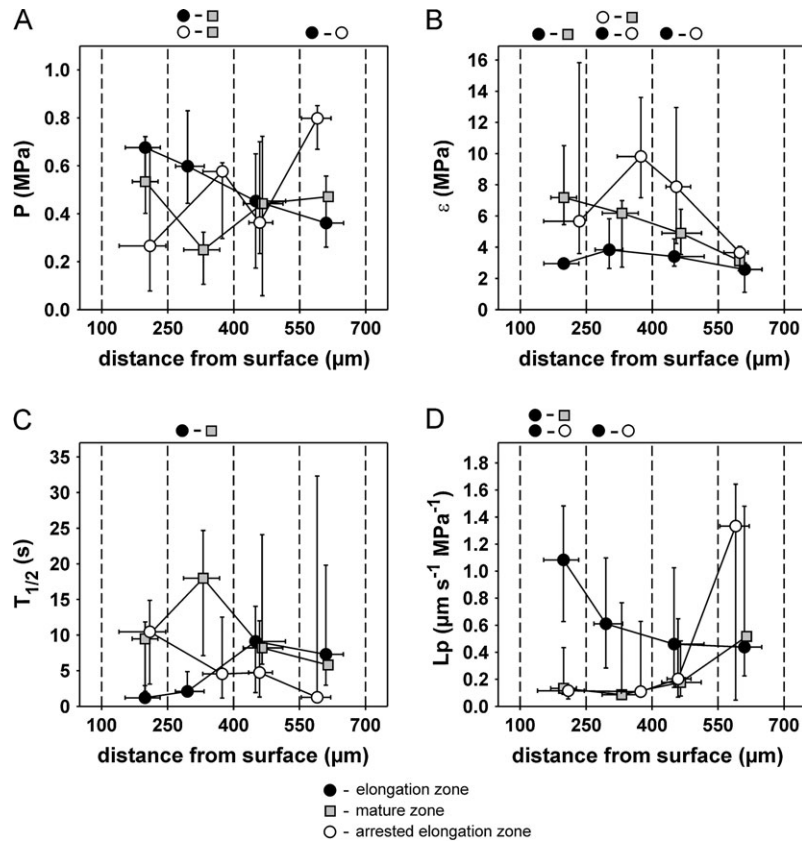


Fig. 6. Radial profile of water relation parameters in the hypocotyl of *Ricinus* seedlings. Water relations parameters (P : turgor; ϵ : elastic modulus; $T_{1/2}$: half-time of pressure relaxation) were measured in cells of the elongation (black circles) and the mature zone (grey squares) of dark-grown seedlings and in the growth-arrested elongation zone of dark-grown seedlings which were illuminated for at least 12 h (white circles). The hydraulic conductivity (L_p) was calculated as described in the Materials and methods. Data points: Median ± 25 (left and down error bars) and 75 percentile (right and up error bars). Statistically significant differences between samples within a specific depth layer are indicated by the symbols above the plots; Statistical test: Mann-Whitney Rank-Sum-Test (two-tailed), all $P \leq 0.05$; $n=28$ (elongation zone), 13 (mature zone), and 26 (elongation zone after illumination), respectively.

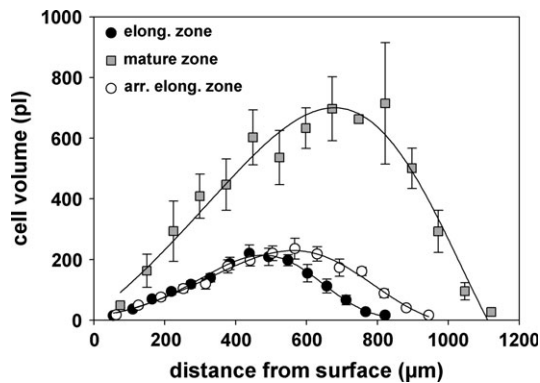


Fig. 7. Radial profile of cell volumes along the cortex of the elongation zone (black circles) and the mature zone (grey squares) of etiolated seedlings and of the arrested elongation zone (white circles) of illuminated seedlings. The measurements were grouped into 15 equidistant depth intervals from the epidermis to the vascular bundle. This arrangement allowed comparison of the results of corresponding cell layers, although the absolute distance from the epidermis varied in the three hypocotyl zones. The trend line of each radial profile was used to select the average cell volume to calculate L_p . The cell volumes are expressed as the mean \pm SE; each of the 15 depth interval contains about 30 measurements from three to four independent plants.

and *RcPIP2-1*, respectively, were abundantly expressed in the castor bean hypocotyl and encode aquaporins of the TIP1 and the PIP2 subgroup (Johanson *et al.*, 2001). The mRNA of each of these genes was increased when cells started to elongate, but only in the case of *RcTIP1-1* and *RcPIP2-1* was the mRNA amount reduced again in mature hypocotyl cells of etiolated seedlings, as shown by RNA gel blot hybridizations. Illumination led to a significant reduction in the amount of *RcPIP2-1* mRNA in the former elongation zone, but did not alter the mRNA amounts of the two other *MIP* genes (Fig. 3; Table 2).

On a protein level, the density of RcPIP2-1 in membranes of the elongation zone was significantly increased and remained high in the mature hypocotyl zone (Fig. 3). In contrast to etiolated seedlings, the RcPIP2-1 protein level in illuminated seedlings is considerably lower in the elongating and mature hypocotyl. At a first glance, the lack of increase of *RcPIP2-1* transcription is in good agreement with the low RcPIP2-1 protein amount. However, these seedlings were grown in the dark for 6 d and should have had comparably high amounts of RcPIP2-1 before the 12 h

illumination. Therefore, RcPIP2-1 protein must have been degraded upon illumination, indicating that the stability of RcPIP2-1 protein is differentially regulated in etiolated and illuminated seedlings. RcTIP1-1 and RcPIP1-1 protein density in microsomal membranes remained almost unchanged along the hypocotyl axis (Fig. 3; Table 2).

RcPIP2-1 aquaporin was detected in parenchymatic cells on the outer side of the large xylem vessels (Fig. 5). Phloem cells, which could be clearly identified by immunostaining using antibodies directed against a phloem-localized sucrose carrier RcSCR1 (Eisenbarth and Weig, 2005), had lower RcPIP2-1 protein amounts (Fig. 5). Small cells close to the protoxylem have been proposed to form one of the important barriers for radial water flow in soybean hypocotyls (Nonami *et al.*, 1997). The presence of RcPIP2-1 in similar cells of the castor bean hypocotyl also suggests that the hydraulic resistance of this tissue is lowered during elongation growth. Although RcPIP2-1 disappears from vascular parenchyma cells in the mature hypocotyl, this aquaporin remains abundant in microsomal preparations from this tissue. Unfortunately, the polyclonal antibody raised against a short peptide of RcPIP2-1 exhibited high background staining which made a clear assessment of the protein distribution, for example in the cortex and pith cells, difficult. Nevertheless, the considerably high *RcPIP2-1* mRNA expression (Fig. 4) and the slight increase of RcPIP2-1 protein (Fig. 5) in cross-sections makes it very likely that peripheral cortex cells also contain this aquaporin. It remains to be investigated, whether post-translational modifications such as phosphorylation of RcPIP2-1 alter the hydraulic conductivity of plasma membranes in the non-elongating, mature hypocotyl.

Peripheral cortex cells of the elongation zone exhibit significantly higher hydraulic conductivities (L_p) compared with cells of the mature hypocotyl and with cells of the growth-arrested elongation zone, which do not elongate in the light. In particular, the inward-directed turgor gradient (high in the periphery, lower towards the vascular bundles) was only found in the elongating hypocotyl and not in non-elongating tissue.

In a previous work, turgor gradients in the opposite direction have been observed in the hypocotyl cortex of castor bean (Meshcheryakov *et al.*, 1992). However, the seedlings used in these experiments were investigated under laboratory light conditions which most likely inhibited hypocotyl elongation (E Komor and E Steudle, personal communication). Interestingly, an average osmotic potential down to -0.8 MPa has been determined previously in the growing and mature castor bean hypocotyl (Balane, 1997). It would be interesting to find out whether peripheral cells exhibit higher osmotic values compared with cells closer to the vascular system. One would expect such high osmotic values in peripheral cells compensating the high turgor and creating a water potential gradient (more negative in the periphery) to allow radial water flow. Because a series of

cells were measured consecutively in these experiments, there was no possibility of analysing the osmotic values of the cells. Further experiments are necessary to measure the osmotic values of the cortical cells which should then permit the calculation of the water potential profile across this tissue.

Since the expression profile of RcPIP2-1 (deduced from mRNA levels and from immunolocalization in vascular parenchyma cells) along the hypocotyl axis and after illumination is closely correlated with the elongation activity of the corresponding cells, this aquaporin is probably the best candidate to be directly involved in facilitating the radial water flow in the elongating hypocotyl.

Because the *Ricinus* seedling is very useful for the molecular analysis of aquaporins and the biophysical analysis using the cell pressure probe, more detailed experiments should be directed to the analysis of the osmotic and mechanic parameters of the growing castor bean hypocotyl. These data should allow an investigation as to what extent of the observed dynamic changes in hydraulic conductivities will affect the hydraulic conductance of the entire tissue.

Acknowledgements

We gratefully acknowledge the help of the following colleagues: Ernst Steudle and Burkhard Stumpf (University of Bayreuth) for their comments and technical advice concerning the cell pressure probe; Ewald Komor (University of Bayreuth) and Wieland Fricke (University of Paisley) for helpful discussions; Rainer Hedrich, Elena Jeworutzki, and Dietmar Geiger (University of Würzburg) for their help with the oocyte injections; Chris Somerville (Stanford University) for providing us with the endosperm-specific cDNA clones. The technical help of Andrea Kirpal and Pia Großmann is also gratefully acknowledged. This work was supported by the Deutsche Forschungsgemeinschaft (grant no. We1680/4 to ARW).

References

- Balane SG. 1997. Regulation des Stärke- und Zuckermetabolismus in der Wachstumszone des Hypokotyls des Rizinuskeimlings. PhD thesis, University of Bayreuth, Germany, Bayreuth.
- Biela A, Grote K, Otto B, Hoth S, Hedrich R, Kaldenhoff R. 1999. The *Nicotiana tabacum* plasma membrane aquaporin NtAQP1 is mercury-insensitive and permeable for glycerol. *The Plant Journal* **18**, 565–570.
- Boyer JS. 2001. Growth-induced water potentials originate from wall yielding during growth. *Journal of Experimental Botany* **52**, 1483–1488.
- Boyer JS, Silk WK. 2004. Hydraulics of plant growth. *Functional Plant Biology* **31**, 761–773.
- Daniels MJ, Mirkov TE, Chrispeels MJ. 1994. The plasma membrane of *Arabidopsis thaliana* contains a mercury-insensitive aquaporin that is a homolog of the tonoplast water channel protein TIP. *Plant Physiology* **106**, 1325–1333.
- Dean RM, Rivers RL, Zeidel ML, Roberts DM. 1999. Purification and functional reconstitution of soybean nodulin 26: an aquaporin with water and glycerol transport properties. *Biochemistry* **38**, 347–353.

- Eisenbarth DA, Weig AR. 2005. Sucrose carrier RcSCR1 is involved in sucrose retrieval, but not in sucrose unloading in growing hypocotyls of *Ricinus communis* L. *Plant Biology* **7**, 98–103.
- Fetter K, Van Wilder V, Moshelion M, Chaumont F. 2004. Interactions between plasma membrane aquaporins modulate their water channel activity. *The Plant Cell* **16**, 215–228.
- Gerbeau P, Guclu J, Ripoche P, Maurel C. 1999. Aquaporin Nt-TIPa can account for the high permeability of tobacco cell vacuolar membrane to small neutral solutes. *The Plant Journal* **18**, 577–587.
- Hanba YT, Shibasaka M, Hayashi Y, Hayakawa T, Kasamo K, Terashima I, Katsuhara M. 2004. Overexpression of the barley aquaporin HvPIP2;1 increases internal CO₂ conductance and CO₂ assimilation in the leaves of transgenic rice plants. *Plant and Cell Physiology* **45**, 521–529.
- Henzler T, Waterhouse RN, Smyth AJ, Carvajal M, Cooke DT, Schäffner AR, Steudle E, Clarkson DT. 1999. Diurnal variations in hydraulic conductivity and root pressure can be correlated with the expression of putative aquaporins in the roots of *Lotus japonicus*. *Planta* **210**, 50–60.
- Hill AE, Shachar-Hill B, Shachar-Hill Y. 2004. What are aquaporins for? *Journal of Membrane Biology* **197**, 1–32.
- Höfte H, Hubbard L, Reizer J, Ludevid D, Herman EM, Chrispeels MJ. 1992. Vegetative and seed-specific forms of tonoplast intrinsic protein in the vacuolar membrane of *Arabidopsis thaliana*. *Plant Physiology* **99**, 561–570.
- Hüsken D, Steudle E, Zimmermann U. 1978. Pressure probe techniques for measuring water relations of cells in higher plants. *Plant Physiology* **61**, 158–163.
- Johanson U, Karlsson M, Johansson I, Gustavsson S, Sjövall S, Frayse F, Weig AR, Kjellbom P. 2001. The complete set of genes encoding major intrinsic proteins in *Arabidopsis* provides a framework for a new nomenclature for major intrinsic proteins in plants. *Plant Physiology* **126**, 1358–1369.
- Johansson I, Karlsson M, Shukla VK, Chrispeels MJ, Larsson C, Kjellbom P. 1998. Water transport activity of the plasma membrane aquaporin PM28A is regulated by phosphorylation. *The Plant Cell* **10**, 451–459.
- Johnson KD, Höfte H, Chrispeels MJ. 1990. An intrinsic tonoplast protein of protein storage vacuoles in seeds is structurally related to a bacterial solute transporter (GlpF). *The Plant Cell* **2**, 525–532.
- Kallarackal J, Orlich G, Schobert C, Komor E. 1989. Sucrose transport into the phloem of *Ricinus communis* L. seedlings as measured by the analysis of sieve-tube sap. *Planta* **177**, 327–335.
- Kammerloher W, Fischer U, Piechotka GP, Schäffner AR. 1994. Water channels in the plant plasma membrane cloned by immunoselection from a mammalian expression system. *The Plant Journal* **6**, 187–199.
- Kinoshita T, Haranishimura I, Siraishi H, Okada K, Shimura Y, Nishimura M. 1994. Nucleotide sequence of a transmembrane protein (TMP-C) cDNA in *Arabidopsis thaliana*. *Plant Physiology* **105**, 1441–1442.
- Köckenberger W, Pope JM, Xia Y, Jeffrey KR, Komor E, Callaghan PT. 1997. A non-invasive measurement of phloem and xylem water flow in castor bean seedlings by nuclear magnetic resonance microimaging. *Planta* **201**, 53–63.
- Ludevid D, Höfte H, Himelblau E, Chrispeels MJ. 1992. The expression pattern of the tonoplast intrinsic protein γ -TIP in *Arabidopsis thaliana* is correlated with cell enlargement. *Plant Physiology* **100**, 1633–1639.
- Maurel C, Chrispeels MJ. 2001. Aquaporins: a molecular entry point into plant water relations. *Plant Physiology* **125**, 135–138.
- Maurel C, Kado RT, Guern J, Chrispeels MJ. 1995. Phosphorylation regulates the water channel activity of the seed-specific aquaporin α TIP. *EMBO Journal* **14**, 3028–3035.
- Maurel C, Tacnet F, Güclü J, Guern J, Ripoche P. 1997. Purified vesicles of tobacco cell vacuolar and plasma membranes exhibit dramatically different water permeability and water channel activity. *Proceedings of the National Academy of Sciences, USA* **94**, 7103–7108.
- Meshcheryakov A, Steudle E, Komor E. 1992. Gradients of turgor, osmotic pressure, and water potential in the cortex of the hypocotyl of growing *Ricinus* seedlings: effects of the supply of water from the xylem and of solutes from the phloem. *Plant Physiology* **98**, 840–852.
- Nonami H, Wu YJ, Boyer JS. 1997. Decreased growth-induced water potential: primary cause of growth inhibition at low water potentials. *Plant Physiology* **114**, 501–509.
- Preston GM, Carroll TP, Guggino WB, Agre P. 1992. Appearance of water channels in *Xenopus* oocytes expressing red cell CHIP28 protein. *Science* **256**, 385–387.
- Quigley F, Rosenberg JM, Shachar-Hill Y, Bohnert HJ. 2002. From genome to function: the *Arabidopsis* aquaporins. *Genome Biology* **3**, research0001.1–0001.17.
- Reizer J, Reizer A, Saier MH. 1993. The MIP family of integral membrane channel proteins: sequence comparisons, evolutionary relationships, reconstructed pathway of evolution, and proposed functional differentiation of the 2 repeated halves of the proteins. *Critical Reviews in Biochemistry and Molecular Biology* **28**, 235–257.
- Sambrook J, Fritsch EF, Maniatis T. 1989. *Molecular cloning: a laboratory manual*. Cold Spring Harbor, NY: Cold Spring Harbor Laboratory Press.
- Schobert C, Komor E. 1989. The differential transport of amino acids into the phloem of *Ricinus communis* L. seedlings as shown by the analysis of sieve-tube sap. *Planta* **177**, 342–349.
- Steudle E. 1997. Water transport across plant tissue: role of water channels. *Biology of the Cell* **89**, 259–273.
- Tang XD, Marten I, Dietrich P, Ivashikina N, Hedrich R, Hoshi T. 2000. Histidine¹¹⁸ in the S2-S3 linker specifically controls activation of the KAT1 channel expressed in *Xenopus* oocytes. *Biophysical Journal* **78**, 1255–1269.
- Tournaire-Roux C, Sutka M, Javot H, Gout E, Gerbeau P, Luu DT, Bligny R, Maurel C. 2003. Cytosolic pH regulates root water transport during anoxic stress through gating of aquaporins. *Nature* **425**, 393–397.
- Tyerman SD, Bohnert HJ, Maurel C, Steudle E, Smith JAC. 1999. Plant aquaporins: their molecular biology, biophysics and significance for plant water relations. *Journal of Experimental Botany* **50**, 1055–1071.
- Uehlein N, Lovisolo C, Siefritz F, Kaldenhoff R. 2003. The tobacco aquaporin NtAQP1 is a membrane CO₂ pore with physiological functions. *Nature* **425**, 734–737.
- van de Loo FJ, Turner S, Somerville C. 1995. Expressed sequence tags from developing castor seeds. *Plant Physiology* **108**, 1141–1150.
- Weig A, Deswarte C, Chrispeels MJ. 1997. The major intrinsic protein family of *Arabidopsis* has 23 members that form three distinct groups with functional aquaporins in each group. *Plant Physiology* **114**, 1347–1357.
- Weig AR, Jakob C. 2000. Functional identification of the glycerol permease activity of *Arabidopsis thaliana* NLM1 and NLM2 proteins by heterologous expression in *Saccharomyces cerevisiae*. *FEBS Letters* **481**, 293–298.